Geophys. J. Int. (2003) **152,** 497–505

On the effects of a dipping axis of symmetry on shear wave splitting measurements in a transversely isotropic medium

Sébastien Chevrot* and Robert D. van der Hilst

Department of Earth, Atmospheric and Planetary Sciences, Massachusetts Institute of Technology, Cambridge, MA 02139, *USA*

Accepted 2002 September 5. Received 2002 March 1; in original form 2001 March 23

SUMMARY

We derive the explicit expressions for the phase velocities and polarizations of quasi-shear waves propagating in a transversely isotropic medium. The normal to the plane defined by the phase normal and the symmetry axis gives the exact polarization of S_1, while the polarization of S_2 also depends on the elastic parameters of the medium and is thus more complicated. Therefore, we propose that the polarization of the slow S_1 wave, instead of the fast S_2 wave, as is common practice, should be determined from seismic data. For a dipping fast axis of symmetry, a 360° periodic variation of the apparent slow axis is predicted, with an amplitude given by $\arctan(\tan\theta/\tan\theta_0)$, where θ is the incidence angle and θ_0 the angle between the symmetry axis and the vertical. For a significant dip of the symmetry axis (larger than 20°) and for large incidence angles these variations should be observable in shear wave splitting measurements. This suggests that *SKKS*, and *S* waves generated by deep earthquakes, which are characterized by larger incidence angles in comparison to *SKS* waves, should be able to constrain a possible dip of the symmetry axis. In contrast, constraining the dip of the symmetry axis from the delay times turns out to be much more difficult owing to their complicated (and non-linear) dependence on azimuth and on the elastic parameters.

Key words: anisotropy, lithosphere, shear wave splitting.

1 INTRODUCTION

Since the pioneering work by Hess (1964), who discovered seismic anisotropy in the oceanic upper mantle, many studies have shown that seismic anisotropy is a general characteristic of the upper mantle under both oceanic and continental regions. It is now well established that lattice-preferred orientation of anisotropic minerals, such as olivine, is one of the principal causes of seismic anisotropy in the upper mantle. Subcontinental anisotropy could be dominated by asthenospheric flow (Vinnik *et al.* 1992) in which case the lineation direction is expected to parallel the absolute plate motion, by a frozen lithospheric fabric developed during the previous orogenic episode (Silver 1996) or by a combination of both (e.g. Levin *et al.* 1999; Levin *et al.* 2000; Fouch *et al.* 2000; Simons *et al.* 2002). Therefore, seismic anisotropy is a potential tool for investigating mantle dynamics and has received considerable attention from seismologists over the previous decade. The most popular and less ambiguous method for studying seismic anisotropy, although it lacks vertical resolution, is the analysis of *SKS* splitting, introduced by Vinnik *et al.* (1984). With this technique one can retrieve an apparent fast direction, which is generally interpreted as the direction of the symmetry axis in the horizontal plane, and a delay time accumulated between the quasi-shear waves during their propagation in the anisotropic medium. The assumption of transverse isotropy (hexagonal symmetry) with a horizontal symmetry axis has been quite successful in explaining most of the shear wave splitting observations (Silver & Chan 1991; Vinnik *et al.* 1992; Silver 1996; Chevrot 2000).

Recently, Zhang & Karato (1995) made some simple-shear deformation experiments on olivine aggregates. They observed that the fast axes of the olivines tend to rotate when the applied deformation increases. For infinite strain, the olivine *a* axes are aligned with the direction of flow, but for intermediate strains the dip of the fast olivine axes is characteristic of the sense of shear. Since simple shear is probably the dominant type of deformation in the asthenosphere, measuring the dip of the symmetry axis could provide crucial constraints on plate–mantle coupling, at least in parts of the mantle where the axis rotation is slow enough. Moreover, if seismic anisotropy is a good indicator of mantle flow, then characterizing the dip of the fast axis is essential in describing its vertical component.

An alternative view is to interpret seismic anisotropy as the manifestation of a palaeofabric frozen in the lithosphere (Silver 1996).

*Now at: Laboratoire de Dynamique terrestre et Planétaire, Observatoire Midi Pyrénées, 31400 Toulouse, France. E-mail: sebastien.chevrot@cnes.fr

Babuška *et al.* (1993) conducted a joint analysis of *P* residuals and *SKS* splitting measurements to infer the orientation of anisotropy. From the bipolar pattern of *P* residuals observed at some stations, they argue that plunging symmetry axes are required. They propose a model of the continental lithosphere characterized by inclined layers of anisotropic structures resulting from the accretion of large blocks of ancient oceanic lithosphere. More recently, Bokelmann (2002) conducted a similar analysis in North America using *P* residuals only. However, the *P* traveltime residuals, which provide the key argument in favour of a dipping orientation of anisotropy, are also sensitive to lateral heterogeneity, which was ignored in their approach. Separating the isotropic and anisotropic contributions to traveltime residuals would require a dense array of seismic stations. Recently, Hartog & Schwartz (2000) made a successful attempt to constrain the dip of the symmetry axis under five stations of the Berkeley Digital Seismic Network using splitting measurements only. Even more complex anisotropic layered structures (with two or even three anisotropic layers with a dipping symmetry axis) were sometimes considered in order to explain shear wave splitting measurements (e.g. Levin *et al.* 1999). In these models it is not clear which features in the data drive the models towards the dipping symmetry axis. Furthermore, a simple physical description of the effects of a dip of the symmetry axis on shear wave splitting measurements is still lacking. In this paper, we show that transversely isotropic (hexagonal) media have special properties that allow such a description.

Determining the analytical expressions of the velocities and polarizations of waves propagating through an anisotropic medium is not trivial. In addition, the general expressions of wave velocities are difficult to interpret and usually bring little physical insight. For these reasons, and also for computational efficiency, perturbation methods have been introduced to derive approximate expressions for wave velocities (Backus 1965; Fedorov 1968; Jech & Pšenčík 1989; Thomsen 1986; Mensch & Rasolofosaon 1997) and wave polarizations (Fedorov 1968; Jech & Pšenčík 1989; Farra 2001) in weakly anisotropic media.

Different approaches have been used to obtain the approximate expressions of phase velocities in transversely isotropic media. Thomsen (1986) determined the general expressions of phase velocities, following Daley & Hron (1977), and considered the case of weak anisotropy to simplify these expressions. Mensch & Rasolofosaon (1997) perturbed the elastic tensor to derive approximate expressions of phase velocities in media of arbitrary symmetry. For a transversely isotropic medium with 8 per cent anisotropy, they show that the approximate velocities deviate from the exact velocities by less than 0.5 per cent. Fedorov (1968) determined the general expressions of the phase velocities from the covariant form of the Christoffel matrix and derived approximate formulae by a perturbation of the Christoffel matrix with respect to a reference isotropic medium obtained by minimizing the norm of the perturbed matrix over all directions.

In this study, we use the perturbation method introduced by Jech & Pšenčík (1989) on the covariant form of the Christoffel matrix given by Fedorov (1968). With this approach the derivations are straightforward and we obtain simple expressions for the velocities and polarizations of waves in weakly transversely isotropic media. From these expressions, variations of the apparent splitting parameters with backazimuth can be predicted for the case of a dipping axis of symmetry compared with the case where the axis of symmetry is horizontal.

2 FIRST-ORDER PERTURBATION FOR THE VELOCITIES AND POLARIZATIONS OF WAVES IN A TRANSVERSELY ISOTROPIC MEDIUM

Let us consider a plane harmonic wave with frequency ω, propagating in the direction $\hat{\mathbf{n}}$ (where the symbol $\hat{}$ over a vector denotes a unit vector) with a displacement vector:

$$\mathbf{u} = U\hat{\mathbf{p}}e^{i\omega(t-\hat{\mathbf{n}}\cdot\mathbf{x}/V)}, \tag{1}$$

where $\hat{\mathbf{p}}$ and $\mathbf{x}$ are the polarization and the position vectors, respectively, U is the displacement amplitude and V is the phase velocity. The displacement vector satisfies the momentum equation for wave propagation in a homogeneous medium:

$$\rho\frac{\partial^2 u_i}{\partial t^2} - c_{ijkl}\frac{\partial^2 u_k}{\partial x_j \partial x_l} = 0, \tag{2}$$

where ρ is the mass density of the medium and c_{ijkl} is the elastic tensor, which are both considered to be constant. The summation convention is assumed for repeated indices. Inserting eq. (1) into eq. (2) and introducing the Christoffel matrix

$$\Gamma_{jk} = \frac{1}{\rho}c_{ijkl}n_i n_l, \tag{3}$$

leads to the so-called Christoffel equation

$$\Gamma_{jk}p_k = V^2 p_j, \tag{4}$$

from which it appears that the square velocity V^2 is an eigenvalue of $\mathbf{\Gamma}$ and $\hat{\mathbf{p}}$ is the associated eigenvector. Therefore, the elastic properties of the medium determine the phase velocities and polarizations of the elastic waves. In the non-degenerate case two quasi-shear waves will propagate in the anisotropic medium, characterized by orthogonal polarizations.

Following the perturbation approach of Jech & Pšenčík (1989), let us determine the velocities and polarizations of the two quasi-shear waves in a weakly transversely isotropic (or hexagonally symmetric) medium. Such a medium possesses a unique symmetry axis, the direction of which is given by the unit vector $\hat{\mathbf{s}}$. Without loss of generality, we choose a coordinate system (x, y, z) such that $\hat{\mathbf{s}}$ is along the vertical axis (Fig. 1). A plane wave propagates in this medium in the direction $\hat{\mathbf{n}} = (n_1, n_2, n_3) = (\sin\theta\cos\phi, \sin\theta\sin\phi, \cos\theta)$. We write the elastic tensor as the sum of a reference isotropic tensor $\boldsymbol{c}^{(0)}$ and an anisotropic tensor $\boldsymbol{c}^{(1)}$, which represents the deviation from the reference isotropic tensor and contains first-order perturbations of the elastic coefficients:

$$\boldsymbol{c} = \boldsymbol{c}^{(0)} + \boldsymbol{c}^{(1)}. \tag{5}$$

Using the Voigt notation with contracted indices C_{IJ} for the fourth-rank elastic tensor c_{ijkl}, the isotropic reference elastic tensor is given by

$$c^{(0)}_{ijkl} = (C_{33} - 2C_{44})\delta_{ij}\delta_{kl} + C_{44}(\delta_{ik}\delta_{jl} + \delta_{il}\delta_{jk}) \tag{6}$$

$$= \lambda\delta_{ij}\delta_{kl} + \mu(\delta_{ik}\delta_{jl} + \delta_{il}\delta_{jk}) \tag{7}$$

The indices I and J of C_{IJ} vary from 1 to 6, following the rule: (11) $\rightarrow$ 1, (22) $\rightarrow$ 2, (33) $\rightarrow$ 3, (23) $\rightarrow$ 4, (13) $\rightarrow$ 5, (12) $\rightarrow$ 6.

Introducing the three dimensionless anisotropic parameters (Mensch & Rasolofosaon 1997)

$$\epsilon = \frac{C_{11} - C_{33}}{2C_{33}} \tag{8}$$

$$\gamma = \frac{C_{66} - C_{44}}{2C_{44}} \tag{9}$$

$$\delta = \frac{C_{13} - C_{33} + 2C_{44}}{C_{33}} \tag{10}$$

the matrix $C^{(1)}$ for weak transverse isotropy can be written as

$$C^{(1)}_{IJ} = \begin{pmatrix} 2\epsilon C_{33} & 2\epsilon C_{33} - 4\gamma C_{44} & \delta C_{33} & 0 & 0 & 0 \\ 2\epsilon C_{33} - 4\gamma C_{44} & 2\epsilon C_{33} & \delta C_{33} & 0 & 0 & 0 \\ \delta C_{33} & \delta C_{33} & 0 & 0 & 0 & 0 \\ 0 & 0 & 0 & 0 & 0 & 0 \\ 0 & 0 & 0 & 0 & 0 & 0 \\ 0 & 0 & 0 & 0 & 0 & 2\gamma C_{44} \end{pmatrix}. \tag{11}$$

Similarly, the Christoffel matrix Γ can be expressed as the sum of two matrices $\Gamma^{(0)}$ and $\Gamma^{(1)}$ defined by

$$\Gamma^{(0)}_{jk} = \frac{1}{\rho} c^{(0)}_{ijkl} n_i n_l \tag{12}$$

$$\Gamma^{(1)}_{jk} = \frac{1}{\rho} c^{(1)}_{ijkl} n_i n_l. \tag{13}$$

Using the theory of invariants (Robertson 1940; Fedorov 1968), $\Gamma^{(0)}$ and $\Gamma^{(1)}$ can be expressed as a linear combination of the dyads that can be formed with the vectors $\hat{\mathbf{s}}$ and $\hat{\mathbf{n}}$ (Fig. 1):

$$\Gamma^{(0)} = (a_0 \mathbf{I} + a_1 \hat{\mathbf{n}} \otimes \hat{\mathbf{n}})/\rho \tag{14}$$

$$\Gamma^{(1)} = [b_0 \mathbf{I} + b_1 \hat{\mathbf{n}} \otimes \hat{\mathbf{n}} + b_2 \hat{\mathbf{s}} \otimes \hat{\mathbf{s}} + b_3 (\hat{\mathbf{s}} \otimes \hat{\mathbf{n}} + \hat{\mathbf{n}} \otimes \hat{\mathbf{s}})]/\rho \tag{15}$$

where $\mathbf{I}$ is the identity matrix, and

$$a_0 = C_{44} \tag{16}$$

$$a_1 = C_{33} - C_{44} \tag{17}$$

$$b_0 = 2\gamma C_{44}\left(n_1^2 + n_2^2\right) \tag{18}$$

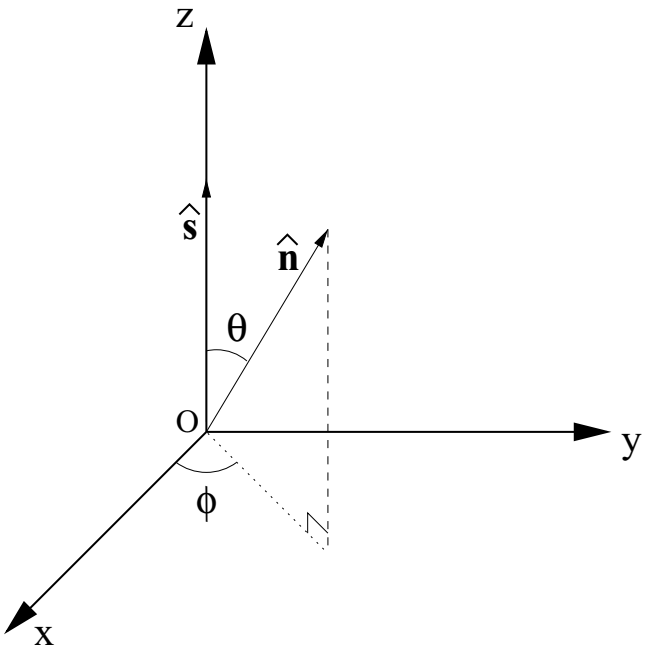

Figure 1. System of coordinate axes. $\hat{\mathbf{s}}$, the symmetry axis, is oriented along the vertical axis. $\hat{\mathbf{n}}$ is the unit phase normal defined by the angles θ and ϕ. θ is the angle between $\hat{\mathbf{s}}$ and $\hat{\mathbf{n}}$.

$$b_1 = 2\epsilon C_{33} - 4\gamma C_{44} \tag{19}$$

$$b_2 = 2\epsilon C_{33} n_3^2 - 2\gamma C_{44} - 2\delta C_{33} n_3^2 \tag{20}$$

$$b_3 = (-2\epsilon + \delta) C_{33} n_3 + 2\gamma C_{44} n_3. \tag{21}$$

The circled cross represents the outer (or tensor) product between two vectors.

2.1 Polarizations

In the reference isotropic medium, the shear waves propagate with the velocity $\sqrt{C_{44}/\rho}$ and are orthogonally polarized in the plane perpendicular to $\hat{\mathbf{n}}$. Two orthogonal unit vectors $\hat{\mathbf{e}}_1 = (e_{11}, e_{12}, e_{13})$ and $\hat{\mathbf{e}}_2 = (e_{21}, e_{22}, e_{23})$ can be chosen arbitrarily in the plane perpendicular to $\hat{\mathbf{n}}$ to describe the polarization $\hat{\mathbf{p}}_1$ and $\hat{\mathbf{p}}_2$ of S_1 and S_2. If $\hat{\mathbf{e}}_1 \cdot \Gamma^{(1)} \cdot \hat{\mathbf{e}}_2 = 0$, the two shear waves are polarized along $\hat{\mathbf{e}}_1$ and $\hat{\mathbf{e}}_2$ in the reference medium (Jech & Pšenčík 1989). After some manipulations, taking into account that the three vectors $\hat{\mathbf{e}}_1$, $\hat{\mathbf{e}}_2$ and $\hat{\mathbf{n}}$ are orthogonal, this condition reduces to

$$e_{13} e_{23} = 0, \tag{22}$$

i.e. either e_{13} or e_{23} is null. Without loss of generality, we can choose $e_{13} = 0$. Therefore, the wave S_1 is in the horizontal plane and is orthogonal to $\hat{\mathbf{n}}$. This uniquely defines the polarization of S_1 described by the unit vector

$$\hat{\mathbf{p}}_1 = \hat{\mathbf{e}}_1 = (-\sin\phi, \cos\phi, 0), \tag{23}$$

which is orthogonal to the plane defined by $\hat{\mathbf{s}}$ and $\hat{\mathbf{n}}$. Since from eq. (15), $\hat{\mathbf{e}}_1 \cdot \Gamma^{(1)} \cdot \hat{\mathbf{n}} = 0$, the perturbation of the polarization of S_1 in the anisotropic medium is 0 and S_1 in the anisotropic medium is polarized along $\hat{\mathbf{e}}_1$. This is an important property of wave propagation in transversely isotropic media, already established by Fedorov (1968) and Helbig (1994): 'At least one of the three waves in any direction within a plane of symmetry is purely transverse with polarization vectors perpendicular to the plane'.

Since the polarization $\hat{\mathbf{p}}_2$ of S_2 in the reference medium is orthogonal to both $\hat{\mathbf{p}}_1$ and $\hat{\mathbf{n}}$, we obtain

$$\hat{\mathbf{p}}_2 = \hat{\mathbf{e}}_2 = (\cos\phi\cos\theta, \sin\phi\cos\theta, -\sin\theta). \tag{24}$$

The three vectors $\hat{\mathbf{n}}$, $\hat{\mathbf{p}}_1$ and $\hat{\mathbf{p}}_2$ are identical to the rows of the rotation matrix used by Mensch & Rasolofosaon (1997) to rotate the elastic tensor and obtain approximate expressions of phase velocities in anisotropic media of arbitrary symmetry. Since $\hat{\mathbf{e}}_1 \cdot \Gamma^{(1)} \cdot \hat{\mathbf{n}} = \hat{\mathbf{n}} \cdot \Gamma^{(1)} \cdot \hat{\mathbf{n}} = 0$, the perturbation of $\hat{\mathbf{p}}_2$ is simply (Jech & Pšenčík 1989)

$$\Delta\hat{\mathbf{p}}_2 = \frac{\hat{\mathbf{e}}_2 \cdot \Gamma^{(1)} \cdot \hat{\mathbf{n}}}{V_S^2 - V_P^2}\hat{\mathbf{n}} = \frac{2\epsilon \sin^3\theta\cos\theta + \frac{1}{2}\delta \sin 2\theta \cos 2\theta}{C_{44}/C_{33} - 1}\hat{\mathbf{n}} = a\hat{\mathbf{n}}. \tag{25}$$

Therefore, the polarizations of the P and S_2 waves in a transversely isotropic medium are obtained by a rotation of $\hat{\mathbf{n}}$ and $\hat{\mathbf{p}}_2$ about the axis $\hat{\mathbf{e}}_1$ with an angle $\arctan a$. In a weakly transversely isotropic medium, this angle is small and the projection of the polarization of S_2 in the horizontal plane is close to the projection of $\hat{\mathbf{p}}_2$.

For a weakly transversely isotropic medium, $\hat{\mathbf{p}}_1$ and $\hat{\mathbf{p}}_2$ give the polarizations of the two quasi-shear waves in the reference medium and form a natural coordinate system where the non-diagonal terms of the Christoffel matrix are first-order quantities compared with the diagonal terms. In a medium with a lower order of symmetry, such as an orthorhombic medium, it is not possible in general to derive approximate expressions for the polarizations that would depend

linearly on first-order perturbations of the elastic tensor, except in the special case of propagation in a symmetry plane.

In the case of a transversely isotropic medium, we have thus established the important result that the polarization vector $\hat{\mathbf{p}}_1$ is always perpendicular to $\hat{\mathbf{n}}$ and $\hat{\mathbf{s}}$ and thus does not depend on the elastic parameters. This is a remarkable property of transversely isotropic media that allows a simple geometrical description of the polarization of S_1.

2.2 Velocities

From the polarization vectors $\hat{\mathbf{p}}_1$ and $\hat{\mathbf{p}}_2$, it is straightforward to determine the phase velocity perturbation (Jech & Pšenčík 1989):

$$\Delta V_i^2 = \hat{\mathbf{p}}_i \cdot \Gamma^{(1)} \cdot \hat{\mathbf{p}}_i. \tag{26}$$

Using eqs (15), (23), (24) and (26) one obtains

$$\Delta V_1^2 = b_0 = 2C_{44}\gamma \sin^2\theta \tag{27}$$

$$\Delta V_2^2 = b_0 + b_2 \sin^2\theta = 2C_{33}(\epsilon - \delta)\sin^2\theta\cos^2\theta. \tag{28}$$

Therefore, the approximate phase velocities for the quasi-shear waves in a weakly transversely isotropic medium are given by

$$V_1 = \sqrt{\frac{C_{44}}{\rho}}(1 + \gamma \sin^2\theta) \tag{29}$$

$$V_2 = \sqrt{\frac{C_{44}}{\rho}}\left[1 + \frac{C_{33}}{C_{44}}(\epsilon - \delta)\sin^2\theta\cos^2\theta\right]. \tag{30}$$

These expressions are identical to those obtained by Mensch & Rasolofosaon (1997).

2.3 Examples

To illustrate the variability of wave propagation in transversely isotropic media, we will apply the approximate expressions obtained for the polarizations and the velocities to three different transversely isotropic media: ice (Fedorov 1968), quartz β (Fedorov 1968) and a transversely isotropic mantle (TIM) that is obtained by mixing the average elastic tensor of olivine given by Kumazawa & Anderson (1968) around the a axis with an isotropic reference mantle characterized by $V_P = 8.0$ km s^{-1} and $V_S = 4.47$ km s^{-1} in the proportions 1/3 and 2/3. This model is a good analogue to the case where the olivine a axes have a strong maximum in their orientation distribution and where the b and c axes form a girdle around the a axis.

Table 1. Elastic coefficients and densities for three transversely isotropic media: ice (from Fedorov 1968, p. 222), quartz β (from Fedorov 1968, p. 222) and TIM (see text). The symmetry axis, which coincides with the (z) axis, is fast for the TI mantle, but is slow for quartz β. For ice, the symmetry axis is fast for P waves but slow for S waves.

	Ice	Quartz β	TI mantle
C_{11}	13.33	116.60	212.80
C_{33}	14.28	110.40	249.18
C_{44}	3.26	36.06	70.47
C_{66}	3.65	49.95	66.72
C_{13}	5.08	32.80	76.24
ρ	0.91	2.65	3.22

This fabric (fabric B in Ben Ismaïl & Mainprice 1998) is by far the most abundant in the rocks of upper-mantle origin that are collected worldwide (D. Mainprice, pers. comm. 2002). The TIM should be comparable to the model used by Hartog & Schwartz (2000). Fig. 2 shows the exact phase velocity of S_1 (open circles) and S_2 (open squares), given by the eigenvalues of eq. (4), and the approximate S_1 (dotted line) and S_2 (dashed line) velocities, given by eqs (29) and (30) for the three TI media described in Table 1. Note the quality of the estimates provided by the approximate expressions for the phase velocities, which are always within 1.5 per cent of the exact phase velocities.

The different behaviours observed for the TI media are easily explained. When the symmetry axis $\hat{\mathbf{s}}$ is a fast axis, then $\gamma < 0$ and V_1 is a decreasing function of θ, the angle between $\hat{\mathbf{s}}$ and $\hat{\mathbf{n}}$. The TIM model (see Fig. 2c) is an example of such a behaviour. The ice (Fig. 2a) and the quartz β (Fig. 2b) are both characterized by a slow symmetry axis for S waves, but for ice $C_{33} > C_{11}$ and the symmetry axis is a fast axis for P waves. The variations of V_2 with respect to θ depend on the sign of $\epsilon - \delta$. For the three media considered, $\epsilon - \delta > 0$. It is interesting to note that if $\epsilon = \delta$, then V_2 does not depend on θ and the phase velocity of the P wave only depends on the elastic parameters C_{11} and C_{33}, while the phase velocities of the S waves only depend on the elastic parameters C_{44} and C_{66}. This is a very special (degenerate) case, almost never observed in natural rocks (see, for example, the compilation made by Thomsen 1986), for which quasi-shear waves velocities are described by only four parameters: C_{33}, C_{44}, ϵ and γ.

For a horizontal symmetry axis (commonly referred to as azimuthal anisotropy) and a small incidence angle ($\theta \approx \pi/2$), the propagation is subvertical and eqs (29) and (30) can be used to predict the delay time δt, which is now routinely measured from *SKS*

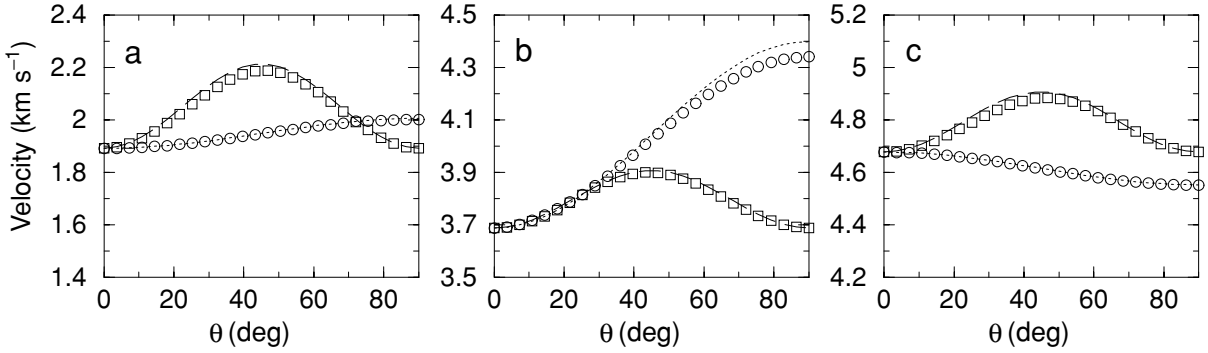

Figure 2. Phase velocities of S_1 (open circles) and S_2 (open squares) waves as a function of θ, the angle between the unit phase normal $\hat{\mathbf{n}}$ and the direction of the symmetry axis $\hat{\mathbf{s}}$ (see Fig. 1) for (a) ice (b) quartz β and (c) TI mantle (see text). The approximate phase velocities given by eqs (29) and (30) for S_1 and S_2 are shown with a dotted line and a dashed line, respectively.

splitting (see Silver, 1996, for a review). The time delay δt, which is the time accumulated between S_1 and S_2, is simply $\delta t = -\gamma t_0$, where t_0 is the time for the shear wave S_2 to propagate through the anisotropic layer.

Whereas model TIM is believed to be a good analogue of the average upper mantle, variations in mineralogy, rock fabric and temperature can induce significant modifications of the elastic tensor, including possibly a loss of symmetry (the effective elastic tensor can become orthorhombic, for example). Alternatively, the characterization of ϵ, γ and δ from shear wave splitting measurements could provide important constraints on the composition and temperature of the upper mantle.

3 PROPAGATION OF SHEAR WAVES IN A TRANSVERSELY ISOTROPIC MEDIUM WITH A DIPPING AXIS OF SYMMETRY

For a subhorizontal symmetry axis and a small incidence angle, the effects on splitting caused by variations of the angle between the symmetry axis and the propagation direction are small and the splitting parameters show no variation with backazimuth. With a good approximation, the behaviour of the quasi-shear waves can then be described as if they were propagating vertically in a TI medium with a horizontal symmetry axis. This implicit assumption is made in almost all the studies based on the analysis of *SKS* splitting. However, when the symmetry axis has a significant dip, systematic variations of the splitting parameters with backazimuth are predicted and become measurable. We describe them in the following section.

3.1 Polarizations

Since the study of *SKS* splitting by Silver & Chan (1991) it has become common practice to measure the horizontal polarization of the fast wave S_2 from seismic records. The results of Section 2.1, however, suggest that a simpler seismic observable is the apparent polarization of the slow S_1 wave since the latter only depends on the dip of the symmetry axis. In a weakly transversely isotropic medium, the assumption that the polarization of S_2 is orthogonal to $\hat{\mathbf{p}}_1$ and $\hat{\mathbf{n}}$ is only approximately verified. For a first-order description of the polarization of S_2 it is necessary to introduce the anisotropic parameters. Therefore, we concentrate on the polarization of S_1 (i.e. the slow wave in a medium such as TIM) in a transversely isotropic medium with a dipping symmetry axis. Let us remark that in the technique introduced by Silver & Chan (1991) the slow polarization can be measured in the same way as the fast polarization.

Let us consider a symmetry axis defined by two angles: the colatitude θ_0 and the longitude or azimuth ϕ_0. Without loss of generality, we can choose a coordinate system such that the symmetry axis is in the xz-plane (Fig. 3). In this coordinate system, $\hat{\mathbf{s}} = (\sin\theta_0, 0, \cos\theta_0)$. The unit propagation vector $\hat{\mathbf{n}}$ is defined by the two polar angles θ and ϕ according to

$$\hat{\mathbf{n}} = (\sin\theta\cos\phi, \sin\theta\sin\phi, \cos\theta). \tag{31}$$

Since $\hat{\mathbf{p}}_1$ is orthogonal to $\hat{\mathbf{s}}$ and $\hat{\mathbf{n}}$, $\hat{\mathbf{p}}_1$ is simply given by

$$\hat{\mathbf{p}}_1 = \frac{\hat{\mathbf{s}} \wedge \hat{\mathbf{n}}}{\|\hat{\mathbf{s}} \wedge \hat{\mathbf{n}}\|}, \tag{32}$$

where the symbol $\wedge$ designates the vector product. Therefore,

$$\hat{\mathbf{p}}_1 = (-\cos\theta_0\sin\theta\sin\phi, -\sin\theta_0\cos\theta + \cos\theta_0\sin\theta\cos\phi, \sin\theta_0\sin\theta\sin\phi)/\|\hat{\mathbf{s}} \wedge \hat{\mathbf{n}}\| \tag{33}$$

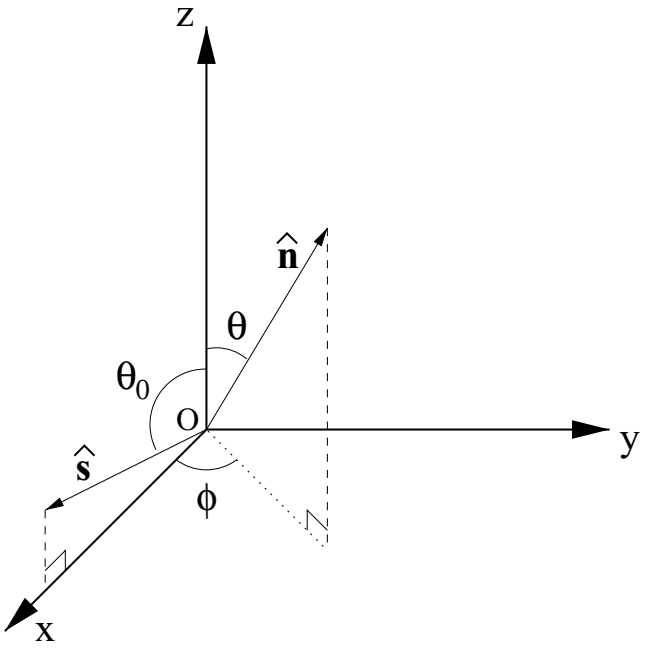

Figure 3. System of coordinate axes. $\hat{\mathbf{s}}$ is the symmetry axis in the (xz)-plane making an angle θ_0 with the vertical axis. The dip of the symmetry axis, defined by the angle that separates the axis direction from the horizontal, is $90 - \theta_0$. $\hat{\mathbf{n}}$ is the unit propagation vector defined by the angles θ and ϕ.

and the polarization of S_1 in the horizontal plane can be described by the vector $\mathbf{p}_1^{\mathrm{h}}$ given by

$$\mathbf{p}_1^{\mathrm{h}} = (-\cos\theta_0\sin\theta\sin\phi, -\sin\theta_0\cos\theta + \cos\theta_0\sin\theta\cos\phi, 0). \tag{34}$$

$\mathbf{p}_1^{\mathrm{h}}$ can be decomposed into a sum of two vectors $\mathbf{r}_0$ and $\mathbf{r}_1$ where

$$\mathbf{r}_0 = (0, -\sin\theta_0\cos\theta, 0) \tag{35}$$

$$\mathbf{r}_1 = (-\cos\theta_0\sin\theta\sin\phi, \cos\theta_0\sin\theta\cos\phi, 0). \tag{36}$$

Should the symmetry axis be horizontal, S_1 would be polarized in the direction $\mathbf{r}_0$. $\mathbf{r}_0$ is along the y axis and does not depend on the azimuth ϕ. On the other hand, for varying azimuths ϕ, $\mathbf{r}_1$ describes a circle of radius $\cos\theta_0\sin\theta$ in the horizontal plane (Fig. 4). As a result, the polarization of the slow and fast quasi-shear waves varies with azimuth. Let us introduce the deviation angle α between the slow axis and the y axis in the horizontal plane. For a horizontal axis of symmetry ($\theta_0 = \pi/2$), or for a vertically incident wave ($\theta = 0$), the magnitude of $\mathbf{r}_1$ is zero and there is no apparent variation of polarization with azimuth ($\alpha = 0$). For a dipping axis of symmetry, α is given by

$$\alpha = \arctan\left(\frac{\sin\phi}{\tan\theta_0/\tan\theta - \cos\phi}\right). \tag{37}$$

The variations of α with azimuth is close to a 360° periodic variation of amplitude $\arctan(\tan\theta/\tan\theta_0)$.

The angular deviation of the apparent slow axis as a function of the azimuth of the incoming S wave is shown in Fig. 5 for a 30° dip of the symmetry axis and three different incident angles: 9° (solid line), 16° (dotted line) and 30° (dashed line). The first angle corresponds to the incidence angle of an *SKS* wave generated by a source at an epicentral distance of 110°. The second angle corresponds to the incidence angle of the *SKKS* wave coming from the same distance. The third angle corresponds to the incidence angle of an S

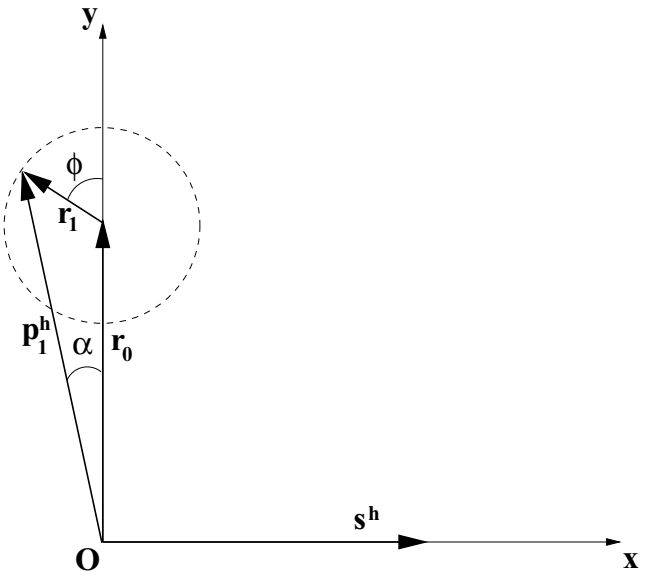

Figure 4. Geometrical representation of $\mathbf{p}_1^{\mathrm{h}}$, the direction of the transverse wave polarization in the horizontal plane. $\mathbf{s}^{\mathrm{h}}$ is the horizontal projection of the symmetry axis on the horizontal plane. $\mathbf{r}_0$ is the polarization that would be observed if the symmetry axis would be horizontal and $\mathbf{r}_1$ is the deviation from this ideal case that results from the dip of the symmetry axis. ϕ is the angle between $\mathbf{r}_0$ and $\mathbf{r}_1$. α is the angular deviation of $\mathbf{p}_1^{\mathrm{h}}$ from $\mathbf{r}_0$.

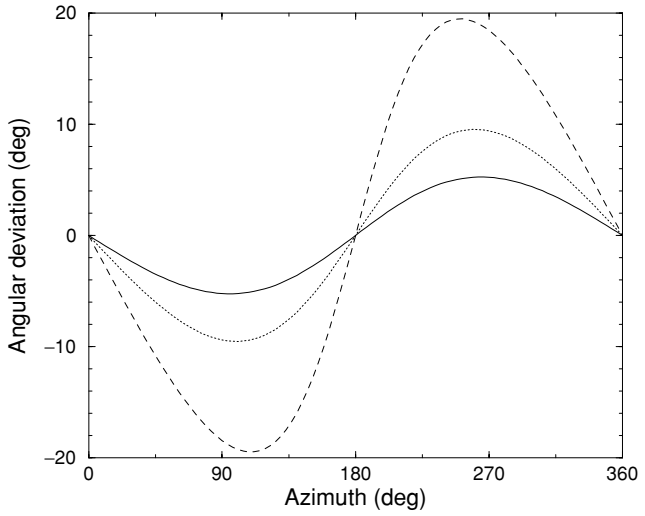

Figure 5. Angular deviation of the transverse wave polarization (angle α in 37) as a function of the backazimuth of the incoming wave for a 30° dip of the symmetry axis for *SKS* (solid line), *SKKS* (dotted line) and *S* (dashed line) waves. For the *S* wave, we have made the assumption that the incoming wave is polarized radially, as for *SKS* and *SKKS*.

wave coming from 60°. The polarizations predicted by eq. (37) are indistinguishable from the polarizations determined from the eigenvectors of eq. (4). The amplitude of the angular deviation shows a clear increase with increasing incidence angles: ∼5°, 9° and 18° for the first, second and third incidence angles, respectively. The angular deviation of the apparent fast axis measured from *SKS* is small, and for most stations would be smaller than the measurement error. However, the angular deviation is doubled with *SKKS* phases, and again doubled with *S* phases. These results imply that in order to constrain the dip of the symmetry axis, shear waves with large incidence angles, such as *S* waves, are needed. If the incidence angle is too large (typically for $\Delta < 40$ for *S* waves), the polarization of shear waves becomes elliptical owing to the overcritical incidence of the *SV* polarized wave at the free surface (Nuttli 1961). Therefore, the epicentral distance range favourable to constrain the symmetry axis dip is approximately between 45° and 80°. Also, in order to avoid any contamination by source-side anisotropy, only deep events (depth >200 km) should be used. Compounding these selection criteria, the uneven distribution of deep seismicity is likely to be the main limitation in determining the dip of the symmetry axis. Following the approach by Chevrot (2000), we construct a map of the azimuthal coverage from deep seismicity given by the hypocentre catalogue of Engdahl *et al.* (1998) (Fig. 6). Briefly, we estimate at each point the number of 10° wide azimuthal windows where teleseisms in the distance range 45°–80° are found, from earthquakes with a hypocentral depth larger than 200 km. The most favourable region seems to be the Central Pacific, with the maximum azimuthal coverage close to Hawaii. Western Australia, Indonesia, Japan, California and India are also characterized by a good azimuthal coverage. On the other hand, the coverage is particularly poor in South America, Africa and western Europe.

3.2 Phase velocities and delay times

Using eqs (29) and (30) and the definitions of $\hat{\mathbf{s}}$ and $\hat{\mathbf{n}}$ it is straightforward to show that for a constant incident angle θ, the approximate phase velocities of the quasi-shear waves as a function of the backazimuth ϕ take the form

$$V_1 = \sqrt{\frac{C_{44}}{\rho}}(A_0 + A_1\cos\phi + A_2\cos 2\phi) \tag{38}$$

$$V_2 = \sqrt{\frac{C_{44}}{\rho}}(B_0 + B_1\cos\phi + B_2\cos 2\phi + B_3\cos 3\phi + B_4\cos 4\phi) \tag{39}$$

with

$$A_0 = 1 + \gamma\left(1 - \frac{1}{2}\sin^2\theta\sin^2\theta_0 - \cos^2\theta\cos^2\theta_0\right) \tag{40}$$

$$A_1 = -\frac{1}{2}\gamma\sin 2\theta\sin 2\theta_0 \tag{41}$$

$$A_2 = -\frac{1}{2}\gamma\sin^2\theta\sin^2\theta_0 \tag{42}$$

$$\begin{aligned} B_0 = 1 + \frac{C_{33}}{C_{44}}(\epsilon-\delta)\Big(&\frac{1}{2}\sin^2\theta\sin^2\theta_0 \\ &+ \cos^2\theta\cos^2\theta_0 - \frac{3}{8}\sin^4\theta\sin^4\theta_0 \\ &-3\sin^2\theta\sin^2\theta_0\cos^2\theta\cos^2\theta_0 - \cos^4\theta\cos^4\theta_0\Big) \end{aligned} \tag{43}$$

$$\begin{aligned} B_1 = \frac{C_{33}}{C_{44}}(\epsilon-\delta)&\sin\theta\sin\theta_0\cos\theta\cos\theta_0 \\ &\times\left(2 - 3\sin^2\theta\sin^2\theta_0 - 4\cos^2\theta\cos^2\theta_0\right) \end{aligned} \tag{44}$$

$$\begin{aligned} B_2 = \frac{C_{33}}{C_{44}}(\epsilon-\delta)\Big(&\frac{1}{2}\sin^2\theta\sin^2\theta_0 - \frac{1}{2}\sin^4\theta\sin^4\theta_0 \\ &-3\sin^2\theta\sin^2\theta_0\cos^2\theta\cos^2\theta_0\Big) \end{aligned} \tag{45}$$

$$B_3 = -\frac{C_{33}}{C_{44}}(\epsilon-\delta)\left(\sin^3\theta\sin^3\theta_0\cos\theta\cos\theta_0\right) \tag{46}$$

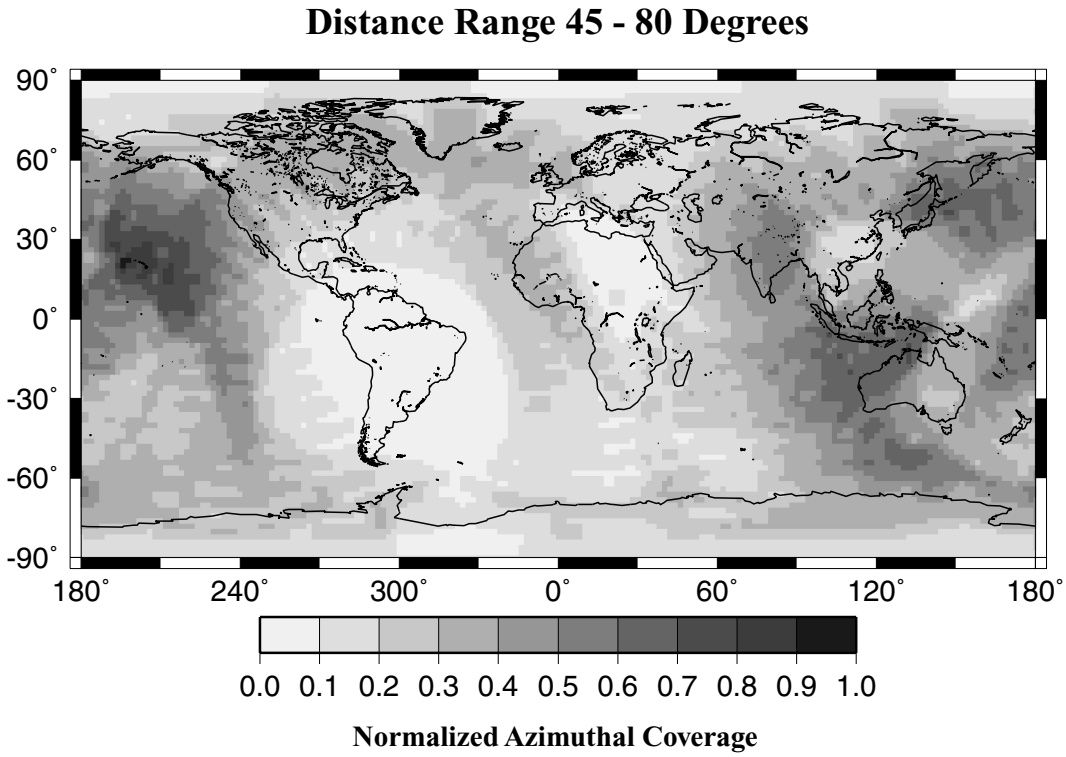

Figure 6. Map of the azimuthal coverage provided by deep earthquakes (depth >200 km) in the distance range 45°–80° (see the text for details).

$$B_4 = -\frac{C_{33}}{C_{44}}(\epsilon - \delta)\left(\frac{1}{8}\sin^4\theta\sin^4\theta_0\right). \tag{47}$$

Similar expressions can be derived for the phase velocities of Love and Rayleigh waves for an arbitrary orientation of the symmetry axis (Montagner & Nataf 1988). For a horizontal axis of symmetry and waves propagating horizontally, $A_1 = 0$ and $B_1 = B_2 = B_3 = 0$. The S_1 wave is polarized vertically and has a phase velocity characterized by a $\cos 2\phi$ dependence on azimuth (Backus 1965; Park 1996), while the S_2 wave has a $\cos 4\phi$ dependence on azimuth.

Care must be taken, however, in the denomination of the two quasi-shear waves. It is a common practice to define *SH* and *SV* waves according to the vertical plane containing the source and the station. The polarization of *SH* is perpendicular to this plane while the polarization of *SV* is in this plane. Here, our convention is different. The propagation of a plane wave in a transversely isotropic medium can be described by two vectors: the wave normal and the symmetry axis. These two vectors, when they are not collinear, define uniquely a plane of symmetry. We have shown that the transverse wave S_1 is always orthogonal to this particular symmetry plane while the radial wave S_2 is polarized in this plane. For a vertical axis of symmetry, all the terms depending on ϕ cancel and the velocities do not depend on azimuth, as expected.

The delay times as a function of azimuth are simply deduced from eqs (38) and (39). For a shear wave with an incidence angle of 10°, a typical angle for an *SKKS* phase, many terms are negligible and the delay time is approximately described by the angular orders 0 and 1:

$$\delta t(\phi) \approx t_0 \left\{\frac{C_{33}}{C_{44}}(\epsilon - \delta)\cos^2\theta_0 - \gamma\sin^2\theta_0 - \frac{1}{2}\sin\right.$$
$$\left.\times\, 2\theta\sin 2\theta_0\left[\gamma + \frac{C_{33}}{C_{44}}(\epsilon - \delta)\cos 2\theta_0\right]\cos\phi\right\}. \tag{48}$$

Therefore, in the case of a dipping axis of symmetry, there is also a 360° periodic variation of the delay time as a function of azimuth. However, the amplitude of this term not only depends on the dip of the symmetry axis but also on the anisotropic parameters ϵ, γ and δ. Therefore, it is complicated to determine θ_0 from the apparent variations of the delay time with azimuth.

4 SINGULAR DIRECTIONS

A first type of singularity is the kiss singularity, where the two slowness surfaces of shear waves touch tangentially, but do not intersect (Crampin & Yedlin 1981). In transversely isotropic media the direction of the symmetry axis always corresponds to a kiss singularity.

The distinction between the quasi-shear waves and the quasi-longitudinal wave from their phase velocities is only meaningful in the case of weak anisotropy. In some 'abnormal' transversely isotropic media (for which $C_{44} + C_{13} < 0$) the transverse wave can propagate faster than the longitudinal wave (Helbig & Schoenberg 1987).

Similarly, TI media exist in which the S_1 wave propagates faster than the S_2 wave. Under these circumstances, the apparent fast axis direction determined from the analysis of shear wave splitting would be orthogonal to the plane containing the actual symmetry axis. A trivial case corresponds to a TI medium in which the symmetry axis is a slow axis. However, some TI media with a fast symmetry axis are characterized by $V_1 > V_2$ in certain propagation directions. This implies that in such media directions for which $V_1 = V_2$ can be found. Such directions are called singular directions (Helbig 1994). For weakly TI media, eqs (29) and (30) give the condition of existence for a singular direction. If the phase velocities of the quasi-shear waves are equal, then

$$\cos^2\theta = \frac{\gamma}{\epsilon - \delta}\frac{C_{44}}{C_{33}}. \tag{49}$$

Therefore, a singular direction exists if $\cos^2\theta < 1$, or if

$$\delta < \epsilon - \frac{C_{44}}{C_{33}}\gamma. \quad (50)$$

This inequality is verified for the ice and the quartz β and the singular directions given by eq. (49) are 73° and 26° away from the symmetry axis, respectively. These directions are very close to the angles at which V_1 and V_2 cross in Figs 2(a) and (b). For the TIM, no singular direction distinct from the symmetry axis exists. If this model accurately describes upper-mantle anisotropy, the apparent fast axis determined from shear wave splitting analysis should always be aligned with the symmetry axis.

5 DISCUSSION AND CONCLUDING REMARKS

We have shown that for a weakly transversely isotropic medium a dipping axis of symmetry produces apparent variations of the polarization of shear waves that are accurately described by eq. (37). For *SKKS* and *S* waves this effect is expected to be well above the measurement uncertainties. In a region characterized by an intermediate strain regime, constraining the dip of the fast axis could provide crucial information concerning plate–mantle coupling (Zhang & Karato 1995) but has so far received little attention from seismologists. The main reason is probably that the dip of the symmetry axis is difficult to measure from *SKS* observations alone. Recently, Hartog & Schwartz (2000) interpreted some splitting measurements made at five stations of the Berkeley Digital Seismic Network in terms of TI with an inclined axis of symmetry. Two of these stations, ORV and CMB, were previously analysed by Savage & Silver (1993). For station ORV, they observed an absence of splitting, while for stations CMB, they determined a 85°E (horizontal) fast axis direction and a delay time of 1.5 s. The latter measurements may not be incompatible with the results obtained by Hartog & Schwartz (2000) who analysed *S* waves from deep earthquakes in addition to *SKS* waves, from which they improved the sensitivity to a possible dip of the symmetry axis. It is very likely that a significant number of stations would benefit from a re-examination of shear wave splitting measurements with these ideas in mind.

In this perspective, the analyst faces two important limitations. The first limitation is the azimuthal coverage provided by natural seismicity. Fig. 6 demonstrates that in places such as South America the measurement of the apparent variations of splitting parameters with azimuth, and thus the determination of dip angle, is almost impossible. The second limitation is the non-uniqueness of single-station splitting measurements interpretations. In particular, it is very difficult to separate the signature of mantle heterogeneity from the dip of the symmetry axis or from the stratification of anisotropy. To overcome this difficulty, the utilization of dense arrays of broadband stations (station spacing less than 50 km) is required. Such detailed analysis of anisotropy should be one of the main objectives of the big seismic stations deployments planned for the future, such as the USArray (Levander *et al.* 1999; Meltzer *et al.* 1999), one of the components of 'EARTHSCOPE'.

ACKNOWLEDGMENTS

Reviews by J. Park and I. Pšenčík improved the manuscript. This research was supported by the David and Lucile Packard Foundation through a fellowship awarded to RH and by the INSU programme 'Intérieur de la Terre'.

REFERENCES

Babuška, V., Plomerová, J. & Šílený, J., 1993. Models of seismic anisotropy in the deep continental lithosphere, *Phys. Earth planet. Inter.,* **78**, 167–191.

Backus, G.E., 1965. Possible forms of seismic anisotropy of the uppermost mantle under oceans, *J. geophys. Res.,* **70**, 3429–3439 (see also comments on this paper by Crampin, S. 1982 and the reply by author the author in, *J. geophys. Res.,* **87,** 4636–4640).

Ben Ismaïl, W. & Mainprice, D., 1998. An olivine fabric database: an overview of upper mantle fabrics and seismic anisotropy, *Tectonophysics,* **296**, 145–157.

Bokelmann, G.H.R., 2002. Convection-driven motion of the North American craton: evidence from *P*-wave anisotropy, *Geophys. J. Int.* **148**, 278–287.

Chevrot, S., 2000. Multichannel analysis of shear wave splitting, *J. geophys. Res.,* **105**, 21 579–21 590.

Crampin, S. & Yedlin, M., 1981. Shear-wave singularities of wave propagation in anisotropic media, *J. Geophys.,* **49**, 43–46.

Daley, P.F. & Hron, F., 1977. Reflection and transmission coefficients for transversely isotropic media, *Bull. seism. Soc. Am.,* **67**, 661–675.

Engdahl, E.R., van der Hilst, R.D. & Bulland, R.P., 1998. Global teleseismic earthquake relocation with improved travel times and procedures for depth determination, *Bull. seism. Soc. Am.,* **88**, 722–743.

Farra, V., 2001. High-order perturbations of the phase velocity and polarization of *qP* and *qS* waves in anisotropic media, *Geophys. J. Int.* **147**, 93–104.

Fedorov, F.I., 1968. *Theory of Elastic Waves in Crystals,* Plenum Press, New York.

Fouch, M.J., Fischer, K.M. & Parmentier, E.M., 2000. Shear wave splitting, continetal keels, and patterns of mantle flow, *J. geophys. Res.,* **105**, 6255–6275.

Hartog, R. & Schwartz, S., 2000. Subduction-induced strain in the upper mantle east of the Mendocino triple junction, California, *J. geophys. Res.,* **105**, 7909–7930.

Helbig, K., 1994. *Foundations of Anisotropy for Exploration Seismics,* Pergamon, Oxford.

Helbig, K. & Schoenberg, M., 1987. Anomalous polarization of elastic waves in transversely isotropic media, *J. acoust. Soc. Am.,* **81**, 1235–1245.

Hess, H.H., 1964. Seismic anisotropy of the uppermost mantle under oceans, *Nature,* **203**, 629–631.

Jech, J. & Pšenčík, I., 1989. First-order perturbation method for anisotropic media, *Geophys. J. Int.* **99**, 369–376.

Kumazawa, M. & Anderson, O.L., 1968. Elastic moduli, pressure derivatives, and temperature derivatives of single-crystal olivine and single-crystal forsterite, *J. geophys. Res.,* **74**, 5961–5972.

Levander, A., Humphreys, G., Ekstrom, G., Meltzer, A. & Shearer, P., 1999. Continental assembly, stability, and disassembly: US array: an Earth sciences initiative to investigate the North American continent, *EOS, Trans. Am. geophys. Un.,* **80**, 245.

Levin, V., Menke, W. & Park, J., 1999. Shear-wave splitting in the Appalachians and the Urals: a case for multilayered anisotropy, *J. geophys. Res.,* **104**, 17 975–17 993.

Levin, V., Menke, W. & Park, J., 2000. No regional anisotropic domains in the northeastern US Appalachians, *J. geophys. Res.,* **105**, 19 029–19 042.

Meltzer, A. *et al.*, 1999. The USArray initiative, *GSA Today,* **9**, 8–10.

Mensch, T. & Rasolofosaon, P., 1997. Elastic-wave velocities in anisotropic media of arbitrary symmetry—generalization of Thomsen's parameters ϵ, δ and γ, *Geophys. J. Int.* **128**, 43–64.

Montagner, J. & Nataf, H., 1988. Vectorial tomography—I. Theory, *Geophys. J.,* **94**, 295–307.

Nuttli, O., 1961. The effect of the Earth's surface on the *S* wave particle motion, *Bull. seism. Soc. Am.,* **51**, 237–246.

Park, J., 1996. Surface waves in layered anisotropic structures, *Geophys. J. Int.* **126**, 173–183.

Robertson, H.P., 1940. The invariant theory of isotropic turbulence, *Proc. Camb. Phil. Soc.,* **36**, 209–223.

Savage, M.K. & Silver, P.G., 1993. Mantle deformation and tectonics: Constraints from seismic anisotropy in the western United States, *Phys. Earth planet. Inter.,* **78**, 207–227.

Silver, P.G., 1996. Seismic anisotropy beneath the continents: probing the depths of geology, *Annu. Rev. Earth Planet. Sci.,* **24**, 385–432.

Silver, P.G. & Chan, W.W., 1991. Shear wave splitting and subcontinental mantle deformation, *J. geophys. Res.,* **96**, 16 429–16 454.

Simons, F.J., van der Hilst, R.D., Montagner, J.-P. & Zielhuis, A., 2002. Multimode Rayleigh wave inversion for heterogeneity and azimuthal anisotropy of the Australian upper mantle, *Geophys. J. Int.* **151**, 738–755.

Thomsen, L., 1986. Weak elastic anisotropy, *Geophysics,* **51**, 1954–1966.

Vinnik, L., Kosarev, G.L. & Makeyeva, L.I., 1984. Anisotropy of the lithosphere from the observations of *SKS* and *SKKS*, *Proc. Acad. Sci. USSR,* **278**, 1335–1339.

Vinnik, L., Makeyeva, L.I., Milev, A. & Usenko, Y., 1992. Global patterns of azimuthal anisotropy and deformations in the continental mantle, *Geophys. J. Int.* **111**, 433–447.

Zhang, S. & Karato, S., 1995. Lattice preffered orientation of olivine aggregates in simple shear, *Nature,* **375**, 774–777.